*Case Report*

# Diagnostic imaging of a large pancreatic pseudocyst with infection over time in a dog

**Chanyoung Ryu[1] Wooseok Jin[1] Sang-Kwon Lee[1] Daji Noh[2] Sooyoung Choi[2] Kija Lee[1*]**

***Abstract***

A 5-year-old Pompitz presented with anorexia and vomiting. Radiographs showed a half-moon-shaped mass in the left cranial abdomen. A large cyst was identified near the left pancreas on ultrasound. Computed tomography revealed a fluid-attenuating mass with rim enhancement in the pancreas. Laboratory tests identified *Staphylococcus warneri* in the cystic lesion, and pancreatic pseudocyst with infection was suspected. The fluid accumulation and clinical signs recurred over several months. Pre-operative magnetic resonance imaging showed a hyperintense cystic lesion with a duct-like structure and hyperintense line between the cyst and the gastric wall on T2-weighted images as well as signal change of the lesion on diffusion-weighted imaging. A partial pancreatectomy was performed, and a pancreatic pseudocyst was confirmed on histopathology. This is a rare case of a large pancreatic pseudocyst from infection with imaging findings in a dog.

**Keywords:** canine, MRI, pancreatic abscess, pancreatic pseudocyst, partial pancreatectomy

[1]*Department of Veterinary Medical Imaging, College of Veterinary Medicine, Kyungpook National University, Daegu 41566, Republic of Korea*

[2]*College of Veterinary Medicine, Kangwon National University, Chuncheon 24341, Republic of Korea*

****Correspondence**: leekj@knu.ac.kr* (K. Lee)

Received: January 26, 2025

Accepted: April 16, 2025

https://doi.org/10.56808/2985-1130.3825

## Introduction

Pancreatic cystic lesions, including pancreatic pseudocyst and abscess, are sequelae following acute pancreatitis (Anderson and Feeney, 2013; Turkvatan *et al*., 2015). A pancreatic pseudocyst is a lesion without an epithelial lining that is filled with fluid containing pancreatic cells and juice surrounded by granulation and fibrous tissue (Coleman and Robson, 2005). There are relatively few reports of characteristic pancreatic cystic lesions in veterinary medicine (VanEnkevort *et al*., 1999; Hwang *et al*., 2018). However, various types of pancreatic pseudocysts and abscesses have been described in human medicine (Zaheer *et al*., 2013; Turkvatan *et al*., 2015). In addition, the imaging classification of pancreatic pseudocysts and abscesses using computed tomography (CT) and magnetic resonance imaging (MRI) and the terminology for complications of pancreatitis have been well established (Balthazar, 2002; Zaheer *et al*., 2013; Turkvatan *et al.* 2015; Morana *et al*., 2021). In this classification scheme, it has been suggested to replace the non-specific term "pancreatic abscess" with the term "pancreatic pseudocyst with infection" when a pancreatic pseudocyst becomes infected and contains pus (Zaheer *et al*., 2013; Turkvatan *et al*., 2015).

We present a case study of a dog affected by a large pancreatic pseudocyst with infection, along with ultrasound, CT, and MRI findings, and outline the course of treatment.

## Case description

A 5-year-old, castrated male Pompitz dog weighing 6.7 kg presented with anorexia and vomiting intensified in the previous three days. Physical examination revealed a "praying position", suggesting abdominal pain. A complete blood cell count revealed a leukocytosis ($65.19 \times 10^9$/L) and neutrophilia ($56.93 \times 10^9$/L). Serum chemistry showed increased lipase (2,493 U/L), canine pancreatic lipase (1,772 U/L), amylase (1,209 U/L), and alkaline phosphatase levels (274 U/L). The blood test and serum chemistry test results are shown in Table 1.

An abdominal radiograph was acquired using a digital radiography system (ACQUIDR; DRGEM, Gyeonggi, Republic of Korea). Abdominal radiography identified a large, soft tissue opacity, half-moon-shaped mass with a smooth contour between the stomach and the left kidney (Fig. 1A). Ultrasound scan of the left cranial abdomen was performed using a 12-MHz linear transducer (Arietta 65; Hitachi Aloka, Tokyo, Japan) with the patient in dorsal recumbency on the table. Abdominal ultrasonography revealed a cyst containing a small amount of echogenic substance with irregular wall thickening located caudomedial to the gastric body (Fig. 1B). The cystic lesion measured approximately 43.6 × 36.4 mm. Irregular thickening (17.0 mm) and hypoechoic parenchyma of the left pancreatic limb, as well as increased echogenicity of the peripheral fat and mild free fluid, were identified (Fig. 1C).

A CT examination was performed using a 64-multislice CT scanner (Aqullion; Canon, Tochigi, Japan). The patient was positioned in dorsal recumbency on the CT table under general anesthesia. The scanning parameters were as follows: 120 kV, 112 mA, 1.0 mm slice thickness, and 0.75 sec rotation time. A contrast study was performed after an intravenous injection of 600 mgI/kg of iohexol (Omnipaque 300 Inj.; GE Healthcare, Chicago, USA) for 20 sec using an autoinjector. Postcontrast CT images of the arterial, portal, and delayed phases were obtained at 20, 45, and 90 sec, respectively, after the contrast medium injection. The CT showed a large fluid-attenuating cystic mass medial to the gastric body that was derived from the distal left pancreatic limb (Fig. 2A). The cystic wall was mildly irregular and showed encapsulation with rim enhancement in the arterial, portal, and delayed phases (Fig. 2B). The stomach was compressed, and the differentiation between the cystic mass and gastric wall was unclear (Fig. 2B). The left pancreatic limb showed gradual enlargement with a lobular border from the proximal to distal part near to the cystic mass. The parenchyma of the left limb was uniformly enhanced and hypoattenuating to the liver during the portal phase.

Considering the lesion size, danger of contamination, and difficulty in approaching the cystic lesion, laparotomic drainage of the cystic lesion was first performed. The fluid from the first drainage attempt was pus. Based on diagnostic imaging, blood biochemistry, and fluid drainage findings, the presumptive diagnosis was a large pancreatic pseudocyst with infection. Routine treatment for pancreatitis and infectious diseases using antibiotics, a synthetic protease inhibitor, and analgesics was pre-emptively applied for the patient. *Staphylococcus warneri (S. warneri)* was identified in a bacterial culture of the purulent fluid. The bacterial infection was sensitive to the previously administered antibiotics, and the patient's clinical symptoms improved. However, 13 days after the laparotomic drainage, anorexia, vomiting, and abdominal pain recurred, and significant fluid accumulation in the pseudocyst was observed on ultrasound. Ultrasound-guided drainage was attempted to improve the clinical signs.

Over the next seven months, ultrasound-guided drainage was performed 32 times due to refilling of the pancreatic pseudocyst. Although the drainage gradually changed from purulent to viscous fluid, the patient's clinical symptoms recurred based on the degree of fluid accumulation, so a surgical approach for the pancreatic pseudocyst was required. On a pre-operative CT scan, a fluid-attenuating, encapsulated lesion with mildly irregular, contrast-enhanced wall thickening was slightly reduced in size (21.2 × 24.3 mm) compared with the initial CT image (Fig. 2C). In addition, the peripheral pancreatic parenchyma showed a fluid-attenuating region near to the cystic lesion on the postcontrast images (Fig. 2C). The contrast enhancement pattern and degree of enhancement of the left pancreatic limb were similar to those on the initial CT scan.

**Table 1** Results of complete blood cell counts and serum chemistry tests

| | Result | Reference | Unit |
|---|---|---|---|
| White blood cells | 65.19 | 6.0–17.0 | $10^9$/L |
| Neutrophils | 56.93 | 3.0–12.0 | $10^9$/L |
| Monocytes | 4.64 | 0.2–1.5 | $10^9$/L |
| Lymphocytes | 3.39 | 1.0–4.8 | $10^9$/L |
| Red blood cells | 9.91 | 5.5–8.5 | $10^{12}$/L |
| Hematocrit | 62.47 | 37.0–55.0 | % |
| Lipase | 2,493 | 200–1,800 | U/L |
| Canine pancreatic lipase | 1,772 | 0–200 | ng/ml |
| Amylase | 1,209 | 500–1,500 | U/L |
| Alanine aminotransferase | 112 | 10–125 | U/L |
| Alkaline phosphatase | 274 | 23–212 | U/L |
| Gamma-glutamyl transferase | 2 | 0–11 | U/L |

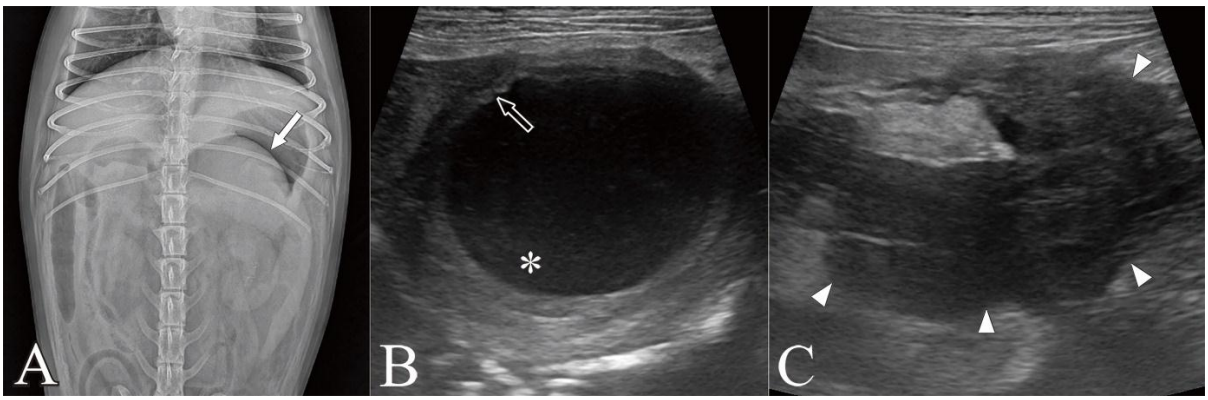


**Figure 1** Ventrodorsal abdominal radiograph (A), abdominal ultrasonographic images (B, C). A smooth, half-moon-shaped, and soft tissue opacity mass (arrow) is visible in the cranial abdomen. A large cyst with a mildly irregular wall (open arrow) and small-volume echogenic contents (asterisk) is located near the left limb of the pancreas. The irregularly thickened left pancreas has heterogeneously hypoechoic parenchyma and hyperechoic peripheral fat (arrowheads).

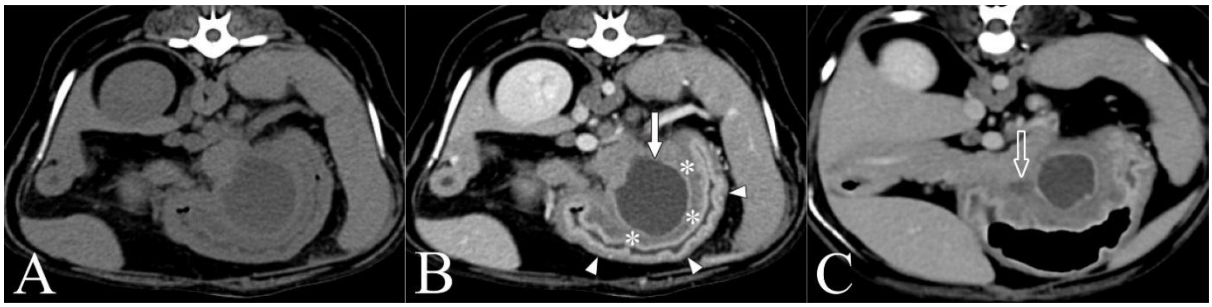


**Figure 2** Non-contrast (A) and delayed phase (B) transverse CT images in the initial stage and delayed phase (C) transverse CT image for the peripancreatic region after seven months. The fluid-attenuating cystic mass (arrow) with rim contrast enhancement is located caudomedial to the lesser curvature of the stomach and originates from the distal left limb of the pancreas. The stomach (arrowheads) is compressed, and the differentiation between the mass and the gastric wall (asterisks) is obscured. The fluid-attenuating region of the left distal pancreatic limb is seen near the cystic lesion, which is smaller than seven months prior (open arrow).

Magnetic resonance imaging (MRI) was performed to further evaluate the affected pancreatic parenchyma and the structure surrounding the pancreatic pseudocyst to be surgically resected. The MRI examination was performed in a 1.5T MRI system (SIGNA Explorer; GE Healthcare, Chicago, USA) with a combination of a 16-channel flex coil. The dog was positioned in dorsal recumbency on the MRI table under general anesthesia. Dorsal T2-weighted images (T2WI) and T1-weighted images (T1WI) of the cranial abdomen, including the pancreas, were acquired. Postcontrast T1WI was obtained immediately after the intravenous administration of 0.15 mmol/kg of gadoterate meglumine (Clariscan; GE Healthcare, Chicago, USA). MRI revealed a pancreatic cystic lesion that was hypointense on T1WI and hyperintense on T2WI (Figs. 3A–C). The cystic wall encapsulating the fluid was hypointense on T2WI, and the internal septation of the wall was faintly enhanced on postcontrast T1WI (Figs. 3A–C). A hyperintense line appeared only along half of the interface between the pancreatic cystic lesion and the serosa of the gastric body on T2WI (Fig. 3C). A duct-like hyperintensity in contact with the wall of the pancreatic cystic lesion was also observed in the distal parenchyma of the left pancreatic limb on T2WI (Fig. 3A). It was obscured that the cystic lesion communicated with the dilated ductal structure. This structure displayed hypointense on diffusion-weighted imaging (DWI) and hyperintense on the corresponding apparent diffusion coefficient

(ADC) map. The cystic lesion was hyperintense on DWI with a b factor of 500 s/mm², whereas its signal intensity was decreased on DWI with a b factor of 1,000 s/mm² (Figs. 3D–E). The ADC value of the cystic lesion was approximately 2.346 × $10^{-3}$ mm²/s (Fig. 3F). The parenchyma of the left pancreatic limb, excluding the cystic lesion, was not enhanced on postcontrast T1WI, and DWI and the ADC map also showed no restricted diffusion.

Based on these MRI findings, a left distal pancreatectomy using an ultrasonic-activated scalpel (UAS) was performed to maximize preservation of the pancreas and removal of the surrounding firm adhesions. The resected cystic lesion was histopathologically diagnosed as a pseudocyst with a fibrous wall without epithelium (Fig. 4). Focally extensive maturing granulation tissue, as well as chronic hemorrhage, were also observed. Four days after the surgery, moderate peritonitis with increased pancreatic enzyme levels in the abdominal free fluid developed. Abnormally increased blood flow in the right pancreatic limb and a concurrent splenic infarction were also observed. Therefore, revision surgery was performed for additional excision of the distal remnant of the left pancreatic limb and the infarcted spleen. Nevertheless, the patient died due to severe peritonitis and ultimately multiple organ failure two days after the revision surgery.

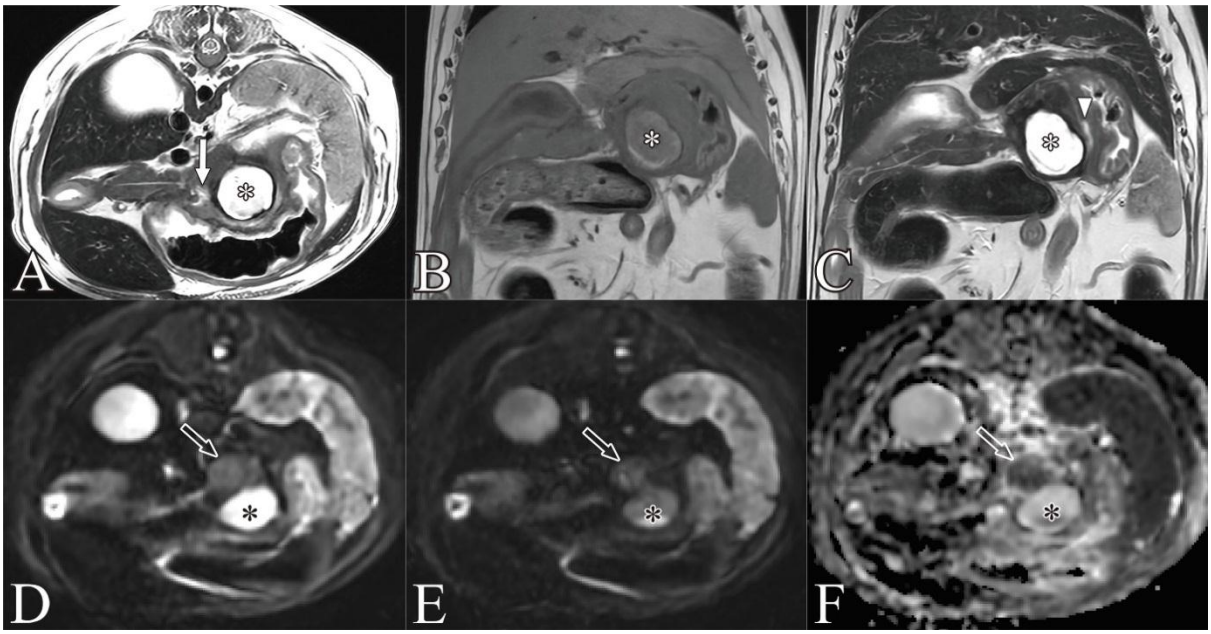


**Figure 3** Transverse T2WI (A), postcontrast dorsal T1WI (B), dorsal T2WI (C), DWI with a b factor of 500 s/mm² (D) and 1,000 s/mm² (E), and ADC map (F). A pancreatic cystic lesion with reduced size (white asterisks) has hypointense and hyperintense contents on T1WI and T2WI, respectively. The cystic wall is faintly enhanced on postcontrast T1WI. The cystic wall and gastric wall are in contact with the hyperintense line (arrowhead) on T2WI. An obscured, duct-like structure (arrow) is identified on T2WI. The cystic lesion (black asterisks) appears hyperintense and isointense compared with the pancreas (open arrows) on DWI with a b factor of 500 s/mm² and 1,000 s/mm², respectively. The ADC map reveals a hyperintense cystic lesion with a high ADC value.

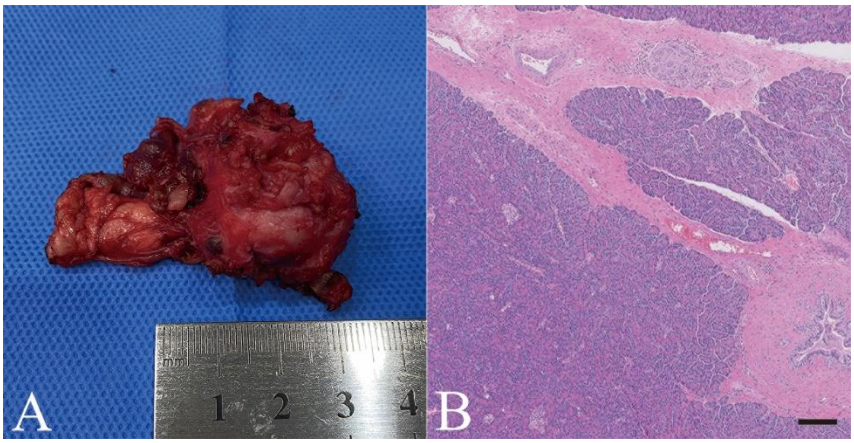


**Figure 4** Postsurgical macroscopic image (A) and histological section (B) of the resected pancreatic lesion. The well-differentiated pancreatic tissue is separated by fibrous trabeculae that extend throughout the pancreatic tissue and surround the outer edge, forming a vague lobular pattern. Haematoxylin and eosin stain; bar = 200 µm.

## Discussion

The choice of treatment modality, medical or surgical, is important for pancreatic fluid accumulations in dogs (Talbot *et al.*, 2022). Although surgical approaches tend to have a high fatality rate, they can be performed in cases of worsening clinical signs, suspicion of sepsis, or biopsy for further diagnosis (Talbot *et al.*, 2022). Ultrasonography is likely to facilitate presurgical awareness of pancreatic fluid accumulation, but it may not be enough to identify pancreatic lesions in dogs. Furthermore, although abdominal ultrasonography can reveal a cystic-like structure and hyperechoic debris as the contents of a pancreatic pseudocyst, the origin of a large cystic lesion may be difficult to determine, and the evaluation also may be affected by the skill of the ultrasonographer (VanEnkevort *et al.*, 1999; Coleman and Robson, 2005; Nemoto *et al.*, 2017). Our case was also identified as a cystic lesion near the pancreas on ultrasonography, but information to specifically identify the lesion was lacking due to its large size characteristic.

CT can facilitate the identification of a pancreatic cystic lesion and its surrounding structures for presurgical planning. In veterinary medicine, CT helps to determine the origin of pancreatic or peripancreatic cystic lesions, and the CT features of pancreatic cystic lesions have been reported in several cases (Nemoto *et al.*, 2017; Hwang *et al.*, 2018; Kim *et al.*, 2021). In our case, the cystic lesion had a clear origin in the left distal pancreas, and the CT features of a single large fluid encapsulation with contents with less than 20 HU of contrast enhancement are similar to those of pancreatic pseudocysts in humans (Turkvatan *et al.*, 2015). However, our case was lacking in significantly increased wall irregularity, wall thickening over time, and air-containing contents of the pancreatic pseudocyst, which differed from the characteristics of infected forms in previously reported human studies (Balthazar, 2002; Zaheer *et al.*, 2013; Turkvatan *et al.*, 2015).

MRI can play an additional role in aiding in the diagnosis of pancreatic pseudocysts. MRI is sensitive for detecting small fluid collections, the pancreatic parenchyma, and the peripheral conditions of pancreatic cystic lesions (Zaheer *et al.*, 2013; Turkvatan *et al.*, 2015; Warda *et al.*, 2015). The MRI features of large pancreatic pseudocysts have not been reported in dogs, but in human medicine, the contents of large pancreatic pseudocysts are hyperintense on T2WI, hypointense on T1WI, and do not have significant signal changes on postcontrast T1WI (Zaheer *et al.*, 2013; Turkvatan *et al.*, 2015). Another previous study comparing pseudocysts and abscesses reported that while abscesses are hyperintense, pseudocysts are isointense to the pancreatic parenchyma on DWI with a b factor of 1,000 s/mm$^2$. The mean ADC value of pseudocysts was $2.8 \pm 0.7 \times 10^{-3}$ mm$^2$/s, and the ADC values of pseudocysts were higher than those of abscesses (Inan *et al.*, 2008). In our study, the signal intensity on T1WI and T2WI and the DWI value of the pseudocysts were similar to the results of the previous human studies (Zaheer *et al.*, 2013; Inan *et al.*, 2008; Turkvatan *et al.*, 2015). In contrast, the pancreatic pseudocyst originating from an abscess, in this case, showed a subtle difference in the internal septations of the wall on postcontrast T1WI. Furthermore, MRI was valuable in evaluating the pancreatic parenchyma and the peripheral area surrounding the pancreatic cystic lesion, including detecting the presence of a duct-like hyperintensity of the distal pancreatic parenchyma in contact with the wall of the pancreatic pseudocyst. Compared with CT, a hyperintense line at the interface between the cystic wall and the serosa of the gastric body was identified on T2WI and suggested the need for surgical treatment to better separate the pancreatic cystic lesion from the surrounding structures. Although not performed in this study, the connection of the main pancreatic duct with a pancreatic cystic lesion could be confirmed through magnetic resonance cholangiopancreatography (MRCP), which is a special MRI technique that obtains images using heavily T2-weighted sequences (Morana *et al.*, 2021). Further study on the MRI features of various pancreatic cystic lesions is needed, and the application of MRCP may better assess pancreatic fluid re-accumulation.

Surgical methods have been developed to prevent the complication of splenic infarction after distal pancreatectomy in human medicine (Beane *et al.*, 2011; Butturini *et al.*, 2012; Kimura *et al.*, 2018). In a patient who underwent laparoscopic spleen-preserving distal pancreatectomy using ultrasonic shears, focal peritonitis from a pancreatic fistula led to a complete splenic infarction; however, this complication spontaneously resolved after one year (Kimura *et al.*, 2018). Our patient required a left distal pancreatectomy, and a laparotomic partial pancreatectomy using a UAS was performed with a spleen-preserving method. We tried to preserve the splenic blood vessels and ligate the pancreatic ductal tributaries by carefully isolating the large pancreatic pseudocyst, but splenic infarction and pancreatic enzyme leakage occurred, similar to the previously reported human study (Kimura *et al.*, 2018). In the present study, the high degree of contact with the surrounding structures of the large pancreatic cystic lesion was another aggravating factor that may have led to splenic infarction; furthermore, focally intense inflammation around the spleen and micro-embolism due to the long operative time of four hours may also have contributed. However, in contrast to the previous human study (Kimura *et al.*, 2018), the dog in the present study died. This may be because the additional excision of the left pancreatic limb to improve the pancreatic leak and the complete resection of the infarcted spleen during the revision surgery were performed too late to resolve the severe peritonitis and splenic infarction.

Canine pancreatic abscesses tend to have negative bacterial cultures (Coleman and Robson *et al.*, 2005; Talbot *et al.*, 2022). In the present study, the initial purulent drainage was positive for *S. warneri* on bacterial culture. *S. warneri* has characteristics of low virulence and slow growth, and after the pre-emptive application of antibiotics in the early stage, an additional culture test may be required (Espino *et al.*, 2006). In our case, with the pre-emptive application of antibiotics, pus was only obtained during the initial laparotomic drainage, and the fluid gradually became a viscous, pancreatic enzyme-enriched fluid after

several drainage procedures. The subsequent aspirations were no longer positive on bacterial cultures, and histology confirmed the resected pancreatic cystic lesion as a pancreatic pseudocyst. As noted above, the findings of this study suggest that initial attempts at fluid aspiration from a pancreatic pseudocyst are necessary in canine patients with suspected bacterial infections and that pancreatic pseudocyst with infection may change into pseudocyst, which is not a common progression.

In conclusion, this report describes the diagnosis and surgical treatment of a pancreatic pseudocyst that resulted from a pancreatic pseudocyst infection in a dog. Diagnostic imaging of large pancreatic cystic lesions provides structural information before invasive treatment. In addition, MRI can provide more useful information regarding adhesion to surrounding structures, the adjacent parenchyma, and the contents of the pancreatic cystic lesion for pre-operative planning. This is the first case report describing MRI findings of a recurrent large pancreatic pseudocyst originating from an *S. warneri*-infected pancreatic pseudocyst in a dog.

***Conflict of interest:*** The authors declare no conflict of interest.

## *References*

Anderson KL and Feeney DA 2013. Diagnostic imaging of the gastrointestinal tract. In: Canine and feline gastroenterology. 1st ed. Washabau RJ, Day MJ (ed). St. Louis: Saunders Elsevier. 205–244.

Balthazar EJ 2002. Complications of acute pancreatitis: Clinical and CT evaluation. Radiol Clin North Am. 40: 1211–1227.

Beane JD, Pitt HA, Nakeeb A, Schmidt CM, House MG, Zyromski NJ, Howard TJ and Lillemoe KD 2011. Splenic preserving distal pancreatectomy: Does vessel preservation matter? J Am Coll Surg. 212: 651–657.

Butturini G, Inama M, Malleo G, Manfredi R, Melotti GL, Piccoli M, Perandini S, Pederzoli P and Bassi C 2012. Perioperative and long-term results of laparoscopic spleen-preserving distal pancreatectomy with or without splenic vessels conservation: a retrospective analysis. J Surg Oncol. 105: 387–392.

Coleman M and Robson M 2005. Pancreatic masses following pancreatitis: Pancreatic pseudocysts, necrosis, and abscesses. Compend Contin Educ Vet. 27: 147–154.

Espino L, Bermudez R, Fidalgo LE, Gonzalez A, Mino N and Quiroga MI 2006. Meningoencephalitis associated with *Staphylococcus warneri* in a dog. J Small Anim Pract. 47: 598–602.

Hwang T, Park S, Lee J, Jung D and Lee HC 2018. Walled-off pancreatic necrosis in a dog. J Vet Clin. 35: 146–149.

Inan N, Arslan A, Akansel G, Anik Y and Demirci A 2008. Diffusion-weighted imaging in the differential diagnosis of cystic lesions of the pancreas. AJR Am J Roentgenol. 191: 1115–1121.

Kim J, Ko J, Yoon H, Kim H, Hwang J, Eom K and Kim J 2021. Clinical and imaging findings of walled-off pancreatic necrosis misdiagnosed as an intra-abdominal neoplasia in a Schnauzer dog: a case report. Vet Med-Czech. 66: 32–39.

Kimura K, Ohira G, Amano R, Yamazoe S, Tanaka R, Tauchi J and Ohira M 2018. A case of complete splenic infarction after laparoscopic spleen-preserving distal pancreatectomy. BMC Surg. 18: 22.

Morana G, Ciet P and Venturini S 2021. Cystic pancreatic lesions: MR imaging findings and management. Insights Imaging. 12: 115.

Nemoto Y, Haraguchi T, Shimokawa Miyama T, Kobayashi K, Hama K, Kurogouchi Y, Fujiki N, Baba K, Okuda M and Mizuno T 2017. Pancreatic abscess in a cat due to *Staphylococcus aureus* infection. J Vet Med Sci. 79: 1146–1150.

Talbot CT, Cheung R, Holmes EJ and Cook SD 2022. Medical and surgical management of pancreatic fluid accumulation in dogs: A retrospective study of 15 cases. J Vet Intern Med. 36: 919–926.

Turkvatan A, Erden A, Turkoglu MA, Secil M and Yuce G 2015. Imaging of acute pancreatitis and its complications. Part 2: Complications of acute pancreatitis. Diagn Interv Imaging. 96: 161–169.

VanEnkevort BA, O'Brien RT and Young KM 1999. Pancreatic pseudocysts in 4 dogs and 2 cats: Ultrasonographic and clinicopathologic findings. J Vet Intern Med. 13: 309–313.

Warda MHA, Hasan DI and Elteeh OA 2015. Differentiation of pancreatic lesions using diffusion-weighted MRI. Egypt J Radiol Nucl Med. 46: 563–568.

Zaheer A, Singh VK, Qureshi RO and Fishman EK 2013. The revised Atlanta classification for acute pancreatitis: Updates in imaging terminology and guidelines. Abdom Imaging. 38: 125–136.